

Flare Associated Oscillations Observed with NoRH

Ayumi ASAI

*Nobeyama Solar Radio Observatory, Minamisaku, Nagano, 384-1305, Nagano, Japan
asai@nro.nao.ac.jp*

Abstract

We present an examination of the multi-wavelength observation of a C7.9 flare which occurred on 1998 November 10. This is an imaging observation of the quasi-periodic pulsations (QPPs) obtained with *Yohkoh*/HXT and Nobeyama Radioheliograph (NoRH). We found that the Alfvén transit time along the flare loop was almost equal to the period of the QPP. We therefore suggest that variations of macroscopic magnetic structures, such as oscillations of coronal loops, affect the efficiency of particle injection/acceleration. We also report other QPP events observed with NoRH, and review some works on these flare-associated oscillations.

Key words: Sun: activity — Sun: flares — Sun: corona — Sun : radio — Sun: X-rays, gammarays

1. Introduction

Associated with solar flares, we often observe nonthermal emissions from high-energy electrons during the impulsive phases. The light curves in such hard X-rays (HXR) and in microwaves show short-lived bursts with durations between 10 s and 10 min (Dulk et al. 1985). These bursts include smaller pulses with shorter duration, and they sometimes show periodicity. A good example of such quasi-periodic pulsations (QPPs) was seen in a flare on 1980 June 7 (Kiplinger et al. 1983; Fig. 1). Nakajima et al. (1983) and Kane et al. (1983) examined the temporal evolution of the HXR and radio spectra and the spatial structure of the flare. They suggest that the QPPs indicate a modulation of the particle injection/acceleration rate. These authors and the followers suggest that the period is comparable to the Alfvén transit time scale.

Asai et al. (2001) examined the QPP using the high resolution HXR and microwave images observed in a solar flare which occurred on 1998 November 10 in NOAA Active Region 8375 (C7.9 on the GOES scale). The flare was observed by *Yohkoh* (Ogawara et al. 1991) and the Nobeyama radio observatory, and clearly showed quasi-periodic behavior in the HXR and microwave time profiles. In the paper we compare the period of the QPP with typical time-scales of flare loops. Then, we discuss the effect of the magnetic structure on the particle injection/acceleration rate. The main parts of the work was already published by Asai et al. (2001) and Grechnev et al. (2003).

We also report the works on flare associated QPPs observed with Nobeyama Radioheliograph (NoRH). These QPP observation can contribute to a new field in the solar physics, called “coronal seismology”. Coronal seismology is an efficient new tool that uses standing MHD waves and oscillations as a tool to explore the physical parameters of the solar corona. Therefore, we review these works on the flare-associated oscillations.

2. 1998 November 10 Flare

2.1. Observations

The solar flare occurred in NOAA 8375 (N19, W78) at 00:10 UT, 1998 November 10. Microwave images of the flare were taken with NoRH (Nakajima et al. 1994). The temporal and the spatial resolutions of the NoRH data are 1.0 s and 12'' (6'') for 17 GHz (34 GHz), respectively. The Nobeyama Radio Polarimeter (NoRP; Torii et al. 1979; Shibasaki et al. 1979; Nakajima et al. 1985) measured the total flux of the flare at 1, 2, 3.75, 9.4, 17, 34 and 80 GHz with a temporal resolution of 0.1 s. The HXR images were obtained with the hard X-ray telescope (HXT; Kosugi et al. 1991) aboard *Yohkoh*, with a spatial and temporal resolution of about 5'' and 0.5 s, respectively. The soft X-ray (SXR) images were also obtained with the *Yohkoh* soft X-ray telescope (SXT; Tsuneta et al. 1991). We used full resolution images in the Partial Frame Image mode with a spatial resolution of about 2''5. We also used magnetogram obtained with the Michelson Doppler Interferometer (MDI; Scherrer et al. 1995) aboard the Solar and Heliospheric Observatory (*SOHO*; Domingo et al. 1995).

Figure 2 shows light curves in the microwave, SXR, and HXR. The top solid line is that of NoRH 17 GHz, the second dotted line is the GOES 1.0 - 8.0 Å channel, the bottom solid line is the HXT M1 band (23 - 33 keV). We can see four bursts in them, and the duration of each burst is a few tens of seconds. The fine spikes in the second burst clearly show the QPPs in both microwaves and HXR. In this paper we investigate the quasi-periodic nature of the second burst.

2.2. Periodic Pulsation

The flare shows a double source in the microwave data. Figure 3 shows the images of NoRH/17 GHz (*grey contours*), the HXT/M1 band (*black contours*), and SXT at the second burst. We refer to the northern and brighter microwave source as the source “A” and the other one as

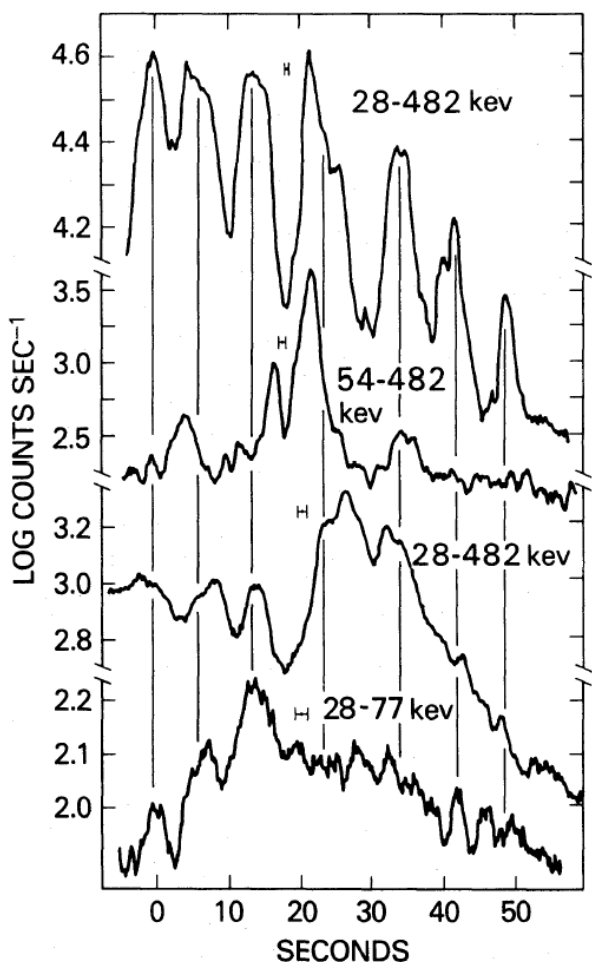


Fig. 1. The impulsive phases of the 1980 June 7 flare (Kiplinger et al. 1983).

source “B”. Although the flare shows double sources in microwave, only source “A” showed the QPP, while the source “B” did not (the right panel of Fig. 4). The period calculated from the autocorrelation function of the time profiles was 6.6 s. On the other hand, in the HXR data only one source is seen near source “B”, which is the “NON-oscillating” microwave source. The background soft X-ray image (*gray scale*) of Figure 3 shows a small bright kernel at the same region at source “B”. We can also see a faint loop which connects the bright kernel and the radio source “A”.

The left panel of Figure 4 presents the HXR and microwave time profiles for the second burst, from 00:14:20 UT to 00:14:40 UT. The QPPs are clearly seen. We also calculated the period of the QPPs in HXR (M1 and M2 bands), and found that the period (6 s) was almost the same as those in NoRP. Analyzing the microwave spectrum using the NoRP data, we confirmed that the emission of QPP originated from optically-thin gyrosynchrotron emission from nonthermal electrons.

To clarify the relation between the microwave QPP at source “A” and the HXR QPP, we investigated in more detail the relationship of the light curves. We calculated

the correlation between the time profiles of 17 GHz and the M1 band as a function of the time lag between them. The maximum correlation was found for a delay of the microwave pulsation with a time of 0.6 - 1.0 s. We suggest that the acceleration site lies near the HXR source, and that the delay time between microwaves and HXRss is explained by the flight duration of nonthermal electrons between both the sources. The projected length of the SXR faint loop is about 5.0×10^4 km. Therefore, if we assume that the velocity of the accelerated electrons is about 1.0×10^5 km s⁻¹ (~ 30 % of the speed of light), then the time delay is comparable to the flight duration of the electrons between both the sources. Hence, it is reasonable to suggest that the acceleration site is located near source “B” and the HXR source, and that the microwave source “A” is generated by the traveled electrons along the faint loop. As the reason why source “B” did not show QPP, we suggest that the emission mechanism of source “B” differs from that of source “A”. From the spectrum, we concluded the dominant emission mechanism of source “B” is thermal Bremsstrahlung.

3. Physical Parameters and Time Scales

Next, we derive some physical parameters of this flare site to discuss the typical timescales of the flare. Temperature, density, size, and magnetic field strength of the flare loop are needed for the estimation.

In the 1998 November 10 flare the length l and width w of the flare loop were derived from the size of flare kernel seen in the SXT images, and they are about 16,000 and 6,000 km, respectively. The temperature T and the volume emission measure EM are derived from the SXT images, by using the filter ratio method (Hara et al. 1992). The average temperature is calculated to be 9.4 MK. Moreover, assuming the volume V from the size of the flare kernel, we derived the number density n in the top of the flare loop of about 4.5×10^{10} (cm⁻³). To measure the magnetic field strength of this region is so difficult because; (1) we can not measure the magnetic field strength of the corona directly, (2) we can not obtain the actual magnetic field strength even in the photosphere at the flare region since it is located near the north-west limb. Therefore, we roughly estimated it by calculating the potential field of the flare region based on a magnetogram on November 6 obtained with *SOHO*/MDI. The field strength on the apex of the flare loop B is estimated to be about 300 G by using the potential field extrapolation (Sakurai 1982).

As a result, the acoustic c_s and the Alfvén c_A velocities are estimated as about 360 and 3,100 km s⁻¹, respectively. Then, the acoustic transit time “along” the flare loop is $\tau_{sl} = l/c_s \approx 44$ s, and the acoustic transit time “across” the flare loop becomes $\tau_{sw} = l/c_s \approx 17$ s. Moreover, the Alfvén transit time “along” the flare loop is $\tau_{Al} = l/c_A \approx 5.1$ s, and the Alfvén transit time “across” the flare loop is $\tau_{Aw} = w/c_A \approx 1.9$ s. The values of our estimations are summarized in Table 1. Although the Alfvén transit time is sensitive to the magnetic field strength estimated above, the transit time along the flare loop (τ_{Al})

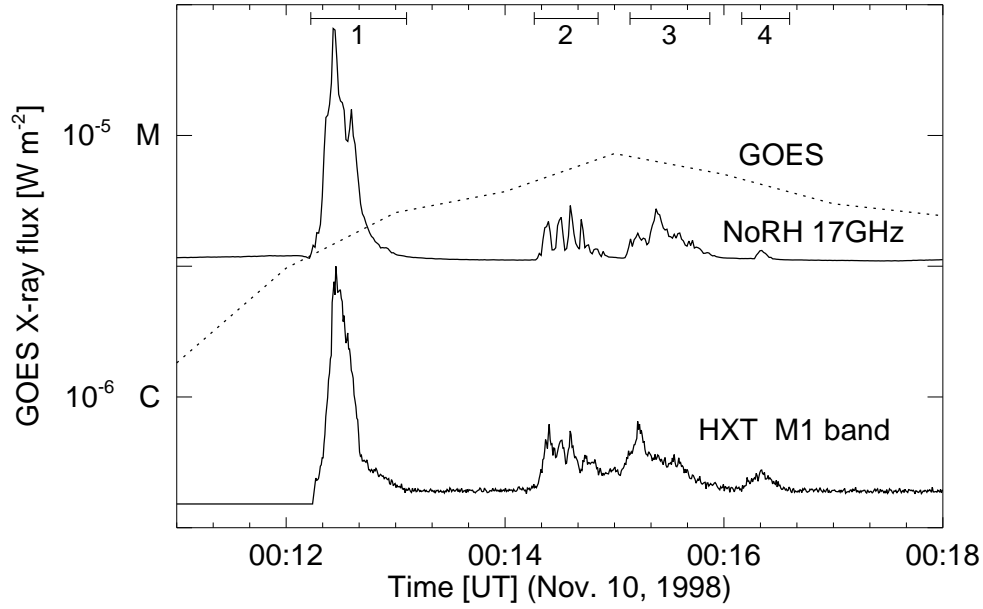


Fig. 2. Temporal evolution of the 1998 November 10 flare. From top to bottom: radio correlation plot observed at 17 GHz with NoRH; soft X-ray flux in the GOES 1.0 - 8.0 Å channel (*dotted line*); hard X-ray count rate measured in the M1 band (23 - 33 keV) of *Yohkoh*/HXT. Four bursts are identified by the numbered top bars.

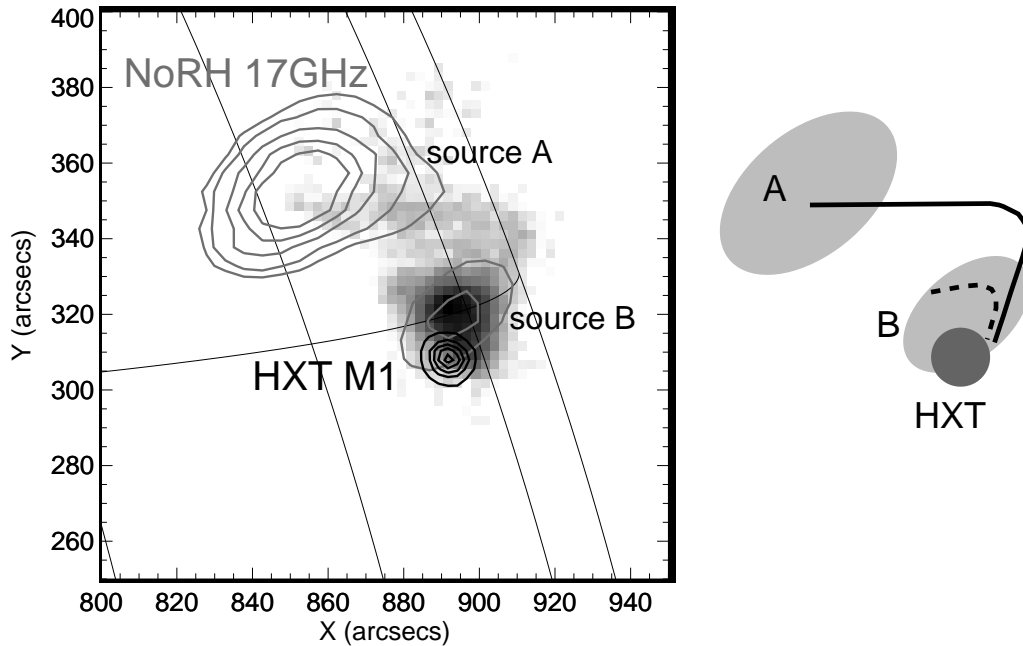


Fig. 3. Left: Coaligned images of the flare in *Yohkoh*SXT (background image), NoRH (17 GHz; *gray contour*) image, and HXT (M1 band) image (*black contour*). Right: a cartoon of this region. The NoRH sources, the HXT source, and SXT faint loop are displayed in light gray, dark gray, and black solid line, respectively. There probably are flare loops (black broken line; see section 3) in microwave source “B” (Asai et al. 2001).

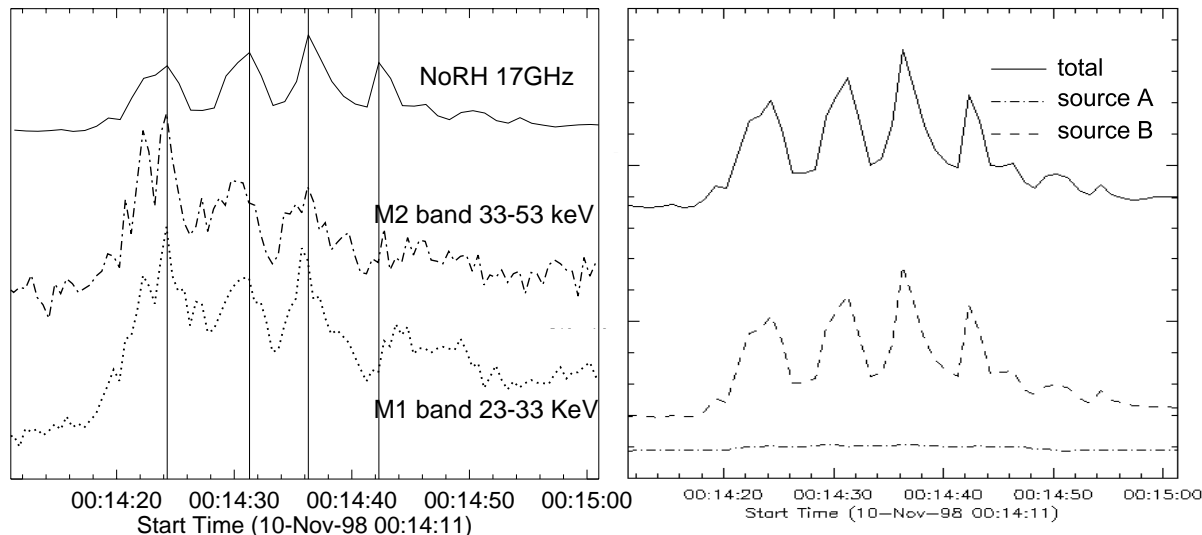


Fig. 4. Left: Light curves of the second burst. From top to bottom: radio brightness temperature observed at 17 GHz by NoRH (solid line); hard X-ray count rate measured in the M2 band (33 - 53 keV) (dash dot line) and M1 band (23 - 33 keV) (dotted line) of *Yohkoh*/HXT. The vertical lines show the peak times of the microwave emission. Right: Light curves of microwave brightness temperature for each emission source.

is the most similar to the observational period of the QPP (6.6 s) in microwave and HXR.

Recently, S. Kamio (in private communication) statistically (4 events in total) examined these QPPs observed with NoRH. They also derived the physical parameters such as temperature, density, magnetic field strength, and so on, as we did. They found that in most case, the Alfvén transit time is the closest to the observed periods of the QPPs. However, there are few events which showed clear QPPs, and there are quite ambiguity on the estimation of the time scales.

4. Oscillation Mode

Now, let us move on the next topic. We found that the QPP period is comparable to the Alfvén transit time scale along the flare loop. From this, we suggest that QPPs are probably occurred by MHD fast mode oscillation. So, we review recent works about the oscillations, and examine which mode is the most reasonable to the observed QPP period.

4.1. Kink mode oscillation

Recently, the observations with the *Transition Region and Coronal Explorer* (*TRACE*; Handy et al. 1999) satellite have shown coronal loop oscillations that was induced by a flare (Nakariakov et al. 1999). The flare loops are shivering because of the disturbance of the flare, and the oscillations are well explained with kink-mode (Aschwanden et al. 1999) whose oscillation period is equal to the Alfvén transit time “along” the oscillating loops (τ_{Al}). The period of observed oscillation is about 300 s. Moreover, Miyagoshi et al. (2004) performed three-dimensional MHD simulations of the coronal loop oscilla-

tion and found that the period of the loop oscillation is also explained with τ_{Al} .

We apply the kink-mode to the case of the 1998 November 10 flare. As we already mentioned, the observed QPP period are the most similar to the transit time along the flare loop (τ_{Al}). Therefore, the kink mode oscillation is the most reliable to explain the QPPs of the flare. However, we have to note that the oscillating loops observed with *TRACE* are much longer and have much weaker magnetic field at their apexes than the QPPs observed with NoRH. It is doubtful whether it is really possible for the flare loops to oscillate clearly and regularly in such circumstances.

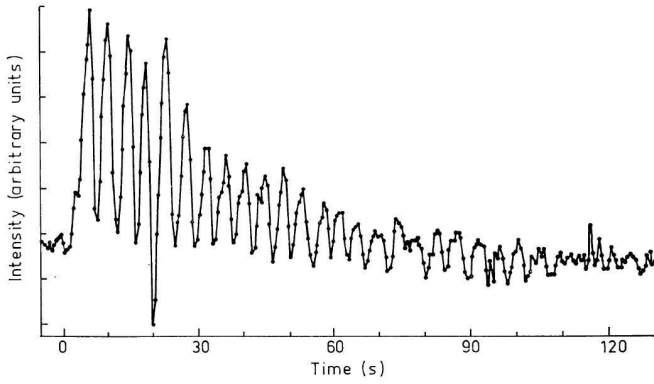
4.2. Sausage mode oscillation

In meric and deci-metric ranges, we can see clear oscillation patterns in their light curves (e.g. McLean & Sheridan 1973). Figure 5 shows an example of the oscillation. Such oscillations with periods of between 0.01 and 1000 sec are sometimes observed associated with solar flares. These oscillations are well explained with the MHD sausage mode.

Nakariakov et al. (2003) reported a QPP event observed with NoRH in the 2000 January 12 event. Although the flare did not show clear QPP in the light curve, they divided the fluctuating component from the smooth component by using Fourier analyses. They also derived other physical parameters on this flare, and then, the fluctuation showed QPP with the period of about 15 second. They discussed which mode corresponds to the oscillation period, by using the physical parameters, and reported that the global sausage mode and the second harmonic mode are the most probable.

Table 1. Physical values of flare loop

Parameter		Value	
volume (V)		4.0×10^{27}	cm^3
length (l)		1.6×10^9	cm
width (w)		$\sim 6.0 \times 10^8$	cm
temperature (T)		9.4×10^6	K
number density (n)		4.5×10^{10}	cm^{-3}
magnetic field (B)		~ 300	G
acoustic velocity (c_s)		3.6×10^2	km s^{-1}
Alfvén velocity (c_A)		3.1×10^3	km s^{-1}
acoustic transit time	along the loop (τ_{sl})	44	s
	across the loop (τ_{sw})	17	s
	along the loop (τ_{Al})	5.1	s
	across the loop (τ_{Aw})	1.9	s

**Fig. 5.** Regular pulses associated with a solar radio outbursts which occurred on 1972 May 16 at a constant frequency of 230 MHz obtained with the Culgoora radio spectrograph. (McLean and Sheridan 1973).

Nakariakov et al. (2003) and Aschwanden et al. (2004) also mentioned on the QPP of the 1998 November 10 flare, and suggested that the sausage mode can explain the oscillation. However, the sausage mode must be higher harmonics, such as 3 or more. We have not answered the question why only the special harmonics number were dominant for the flare.

Although we have only 4 clear QPP events observed with NoRH, we can probably find much more QPP events, by using their method.

5. Loop Oscillation & Particle Acceleration

Finally, we discuss about the relation between the QPP and particle acceleration. The QPP periods probably show that they are generated by the MHD fast mode oscillation (kink mode and/or sausage mode). Does the oscillation of the coronal loop relate with the particle acceleration/injection?

Tajima, Brunel, & Sakai (1982) showed by numerical simulation that stored magnetic energy is explosively transformed to particle acceleration. They also suggest

that the current loop coalescence instability induces the QPPs. Moreover, Tajima et al. (1987) showed that the period of the QPP is equal to the Alfvén transit time “across” the current loop (τ_{Aw}). Although these works were mainly based on the total flux, and the detailed spatial configuration of the flare that shows QPP is still unknown, their work connects the flare loop oscillation and the QPP.

Tsuneta & Naito (1998) propose that nonthermal electrons can efficiently be accelerated by a first order Fermi process at the fast shock located below the reconnection X-point. They suggest that the accelerated electrons are trapped between the two slow shocks, and that the energy injection depends on the length of the fast shock which is pinched by these slow shocks. If the reconnected (flare) loop that is located under the fast shock is oscillating, that the length of the fast shock probably varies with the loop oscillation, synchronously. Hence, we propose, under the hypothesis of the acceleration model proposed by Tsuneta & Naito (1998), that the origin of the QPP in microwaves and HXRs is the modulation of the acceleration/injection of nonthermal electrons. Moreover, we propose that the modulation is produced by the variations of macroscopic magnetic structures, for example, oscillations of coronal loops.

6. Summary & Conclusions

We investigated the impulsive phase of the flare whose time evolution showed a clear QPP in microwaves and HXRs. We found the periods of the QPP, and we estimated some typical time scales of the flare loop from the observational data. We found that the Alfvén transit time along the flare loop was close to the QPP periods in most cases.

Both the kink mode and sausage mode have possibilities to explain the oscillation. Although it is not fixed yet, if we can fix it, the QPPs can become a very useful measure for the coronal seismology. Loop oscillation probably modulates the efficiency of particle acceleration, so we should know how it works, as future works.

References

- Asai, A., Shimojo, M., Isobe, H., Morimoto, T., Yokoyama, T., Shibasaki, K., Nakajima, H. 2001, *ApJL*, 562, L103
- Aschwanden, M. J., Fletcher, L., Schrijver, C. J., Alexander, D. 1999, *ApJ*, 520, 880
- Aschwanden, M. J., Nakariakov, V. M., Melnikov, V. F. 2004, *ApJ*, 600, 458
- Domingo, V., Fleck, B., Poland, A. I. 1995, *Sol. Phys.*, 162, 1
- Dulk, G. A., McLean, D. J., Nelson, G. J. 1985, in *Solar Radiophysics: Studies of emission from the sun at metre wavelengths*, eds. McLean D. J. & Labrum N. R. (Cambridge: Cambridge University Press), 53
- Grechnev, V. V.; White, S. M.; Kundu, M. R. 2003, *ApJ*, 588, 1163
- Handy, B. N., et al. 1999, *Sol. Phys.*, 187, 229
- Hara, H., Tsuneta, S., Lemen, J. R., Acton, L. W., McTiernan, J. M. 1992, *PASJ*, 44, 135
- Kane, S. R., Kai, K., Kosugi, T., Enome, S., Landecker, P. B., McKenzie, D. L. 1983, *ApJ*, 271, 376
- Kiplinger, A. L., Dennis, B. R., Frost, K. J., Orwig, L. E. 1983, *ApJ*, 273, 783
- Kosugi, T., et al. 1991, *Sol. Phys.*, 136, 17
- McLean, D. J., and Sheridan, K. V. 1973, *Sol. Phys.*, 32, 485
- Miyagoshi, T., Yokoyama, T., Shimojo, M. 2004, *PASJ*, 56, 207
- Nakajima, H., Kosugi, T., Kai, K., Enome, S. 1983, *Nature*, 305, 292
- Nakajima, H., et al. 1985, *PASJ*, 37, 163
- Nakajima, H., et al. 1994, *Proc. of the IEEE*, 82, 705
- Nakariakov, V. M., Ofman, L., DeLuca, E. E., Roberts, B., Davila, J. M. 1999, *Science*, 285, 862
- Nakariakov, V. M., Melnikov, V. F., Reznikova, V. E. 2003, *aap*, 412, L7
- Ogawara, Y., Takano, T., Kato, T., Kosugi, T., Tsuneta, S., Watanabe, T., Kondo, I., & Uchida, Y. 1991, *Sol. Phys.*, 136, 10
- Sakurai, T. 1982, *Sol. Phys.*, 76, 301
- Scherrer, P. H., et al. 1995, *Sol. Phys.*, 162, 129
- Shibasaki, K., Ishiguro, M., Enome, S. 1979, in *Proc. of the Res. Inst. of Atmospheric, Nagoya Univ.*, 26, 117
- Tajima, T., Brunel, F., and Sakai, J. 1982, *ApJ*, 258, L45
- Tajima, T., Sakai, J., Nakajima, H., Kosugi, T., Brunel, F., Kundu, M. R. 1987, *ApJ*, 321, 1031
- Torii, C., Tsukiji, Y., Kobayashi, S., Yoshimi, N., Tanaka, H., Enome, S. 1979, in *Proc. of the Res. Inst. of Atmospheric, Nagoya Univ.*, 26, 129
- Tsuneta, S., et al. 1991, *Sol. Phys.*, 136, 37
- Tsuneta, S., and Naito, T. 1998, *ApJ*, 495, L67